Deep Learning for ISAC-Enabled End-to-End Predictive Beamforming in Vehicular Networks

Zihuan Wang and Vincent W.S. Wong
Department of Electrical and Computer Engineering, The University of British Columbia, Vancouver, Canada
email: {zihuanwang, vincentw}@ece.ubc.ca

***Abstract*—Integrated sensing and communications (ISAC) has emerged as a promising technology for predictive beamforming design in vehicle-to-infrastructure (V2I) networks. Most of the existing works use a two-step approach for predictive beamforming design. The first step is to estimate the state parameters of a vehicle (e.g., angle of arrival (AoA), channel state information (CSI)) from the received sensing signal samples at the road side unit (RSU). The second step is to determine the beamforming vector based on the estimated parameters. However, estimation errors may be introduced in the first step which impacts the subsequent beamforming design and leads to degradation in the achievable rate. In this work, by using deep learning, we propose an ISAC-enabled end-to-end predictive beamforming (E2E-PB) approach to obtain the beamforming vector directly from the reflected signal samples. The proposed approach does not require an intermediate state parameters estimation step. We develop an attention-based long short-term memory (LSTM) network to capture the temporal correlation in the reflected signal samples and determine the beamformer. The network is trained in an unsupervised manner to maximize the achievable rate. We compare our proposed E2E-PB approach with two state-of-the-art schemes, namely, the extended Kalman filtering framework and a deep learning based two-step approach. The results show that our proposed E2E-PB approach obtains a higher achievable rate than the other two baseline schemes, and has close performance when compared with the optimal beamforming design with perfect CSI.**

I. Introduction

The sixth-generation (6G) wireless networks are expected to support various emerging applications and use cases. Applications such as autonomous and connected vehicles require both wireless connectivity and sensing capability [1]–[3]. The use of higher frequency bands and larger antenna arrays facilitates the implementation of sensing by utilizing wireless network infrastructures. 6G wireless networks are expected to become perceptive, which stimulates the development of integrated sensing and communications (ISAC) techniques [4], [5]. ISAC integrates the sensing and communications functionalities into a single system, and enables these two modules to share the same hardware and spectrum. The coexistence of sensing and communications can reduce hardware cost, introduce new services, and improve spectral and energy efficiencies.

One of the key applications of ISAC is predictive beamforming design in vehicle-to-infrastructure (V2I) networks. Conventionally, the road side unit (RSU) periodically transmits pilot signals to a vehicle using different beamformers [6]. The vehicle sends the index of the beamformer that achieves the highest rate back to the RSU. However, the conventional approach incurs a high signaling overhead since pilot signals and feedback between the RSU and the vehicle are required. By employing ISAC, the beamformer can be determined based on the sensing signals reflected by the vehicles, such that the pilot signals and feedback overhead can be eliminated.

We now summarize some of the recent works on ISAC-enabled predictive beamforming design in V2I networks. In [6], an extended Kalman filtering framework for predictive beamforming is proposed. First, the state parameters (e.g., angle of arrival (AoA)) of a vehicle are estimated using the reflected signal samples at the RSU. After that, the predictive beamforming is determined based on the estimation results. In [7], a factor graph based message passing algorithm is developed to estimate the state parameters of a vehicle, based on which the beamforming vector is designed. In [8], the position of a vehicle is first predicted based on the reflected signal samples. Then, the beamforming vector is determined given the position information. Besides the aforementioned optimization-based approaches, deep learning based algorithms have also been proposed for predictive beamforming in V2I networks. A deep neural network is developed in [9] to extract the historical angular information of a vehicle from the reflected signal samples. Then, the AoA of the vehicle is estimated, and the beamformer is designed to align with the AoA for the maximization of the achievable rate. A historical channels-based convolutional long short-term memory (LSTM) network is proposed in [10] for predictive beamforming in V2I networks. The historical channel state information (CSI) is first estimated by the RSU. The neural network takes the estimated historical CSI as input and determines the beamforming vector.

The aforementioned works on ISAC-enabled predictive beamforming design include two steps. The first step is to estimate the state parameters of a vehicle (e.g., AoA, CSI) given the reflected signal samples. The second step is to design a beamformer based on the estimated parameters to maximize the achievable rate. However, the two-step approach may not be optimal. This is because estimation errors can be introduced in the first step. The propagation of error may impact the subsequent beamforming design and degrade the achievable rate. To overcome this limitation, in this paper, we develop an end-to-end approach for predictive beamforming, which aims to maximize the achievable rate, while bypassing the intermediate state parameters estimation step. The main contributions of this paper are summarized as follows:

- We propose an ISAC-enabled end-to-end predictive beamforming (E2E-PB) approach for V2I networks. The proposed E2E-PB approach learns an end-to-end mapping between the reflected signal samples and beamformer through neural networks. We apply an unsupervised learning framework for network training to directly maximize the achievable rate of the vehicle.
- We develop an attention-based LSTM network to extract the temporal correlation in the reflected signal samples. The output of the network corresponds to the beamforming vector. The use of attention mechanism enables the network to capture the most important temporal features in the reflected signal samples.
- We conduct simulation experiments to evaluate the performance of the proposed E2E-PB approach. We compare our proposed approach with two state-of-the-art algorithms, namely, the extended Kalman filtering framework [6] and the deep learning based two-step design approach [9]. The results show that our proposed approach provides a higher achievable rate than the baseline schemes. Our proposed approach also achieves close-to-optimal performance when compared with the optimal beamforming design with perfect CSI.

The rest of this paper is organized as follows. The system model and problem formulation for ISAC-enabled predictive beamforming design are presented in Section II. In Section III, we present our proposed E2E-PB approach for V2I networks. Performance evaluation and comparison are shown in Section IV. Conclusions are drawn in Section V.

Notations: We use boldface lower case letters and boldface upper case letters to denote vectors and matrices, respectively. $(\cdot)^*$, $(\cdot)^{\mathrm{T}}$, and $(\cdot)^{\mathrm{H}}$ are used to denote the conjugate, transpose, and conjugate transpose of a vector or matrix, respectively. $\mathbb{C}^N$ and $\mathbb{R}^N$ denote the sets of N-dimensional vectors with complex entries and real entries, respectively. $\mathcal{CN}(\boldsymbol{\mu}, \boldsymbol{\Sigma})$ denotes the complex Gaussian distribution, where $\boldsymbol{\mu}$ and $\boldsymbol{\Sigma}$ are the mean vector and covariance matrix, respectively. $\mathbf{I}_N$ indicates an identity matrix of size N. We use j to denote the imaginary unit which satisfies the equation $j^2 = -1$. $\mathrm{Re}(\cdot)$ and $\mathrm{Im}(\cdot)$ extract the real part and imaginary part of a complex number, respectively. We use $\mathbb{E}\{\cdot\}$ to denote the expectation of a random variable.

II. System Model and Problem Formulation

Consider a V2I network with one RSU communicating with a single-antenna vehicle in a road segment. The RSU has separate antenna arrays with N_{t} transmit antennas and N_{r} receive antennas, which are used for downlink transmission and the reception of the reflected echo signals, respectively. The RSU operates at the millimeter wave (mmWave) frequency band and communicates with the vehicle through a line-of-sight (LoS) path. The RSU communicates with the vehicle for a time period T. We divide the time period T into $N+1$ time slots. The duration of each time slot is ΔT. We consider multiple-input multiple-output (MIMO) uniform linear array (ULA) is adopted at the RSU. The transmit and receive steering vectors are as follows:

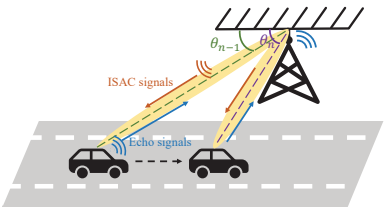

Fig. 1. System model for the considered V2I network.

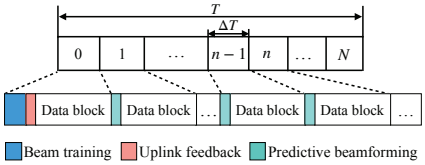

Fig. 2. Frame structure of ISAC-enabled predictive beamforming.

$$\mathbf{a}(\theta_n) = \frac{1}{\sqrt{N_{\mathrm{t}}}} \left[1 \quad e^{-j\pi\cos\theta_n} \quad \cdots \quad e^{-j\pi(N_{\mathrm{t}}-1)\cos\theta_n}\right]^{\mathrm{T}}, \tag{1}$$

$$\mathbf{b}(\theta_n) = \frac{1}{\sqrt{N_{\mathrm{r}}}} \left[1 \quad e^{-j\pi\cos\theta_n} \quad \cdots \quad e^{-j\pi(N_{\mathrm{r}}-1)\cos\theta_n}\right]^{\mathrm{T}}, \tag{2}$$

where θ_n is the AoA in the n-th time slot. By exploiting full-duplex radio technologies, the RSU can receive the echo signals reflected by the vehicle for sensing while maintaining downlink transmissions simultaneously [11]. The system model for the considered V2I network is shown in Fig. 1[1].

The frame structure of the ISAC-enabled predictive beamforming is shown in Fig. 2. Similar to other recent works on vehicle tracking (e.g., [6]–[8]), we assume that the state parameters of the vehicle and the CSI remain constant during each time slot. When the vehicle is within the coverage of the RSU, the RSU first establishes a communication link with the vehicle through conventional beam training and uplink feedback [6] in time slot 0. When a communication link is established, the RSU transmits ISAC signals to the vehicle for downlink transmission and receives the reflected echo signals simultaneously. By using ISAC techniques, the RSU can predict the beamformer for the transmission in the n-th time slot, where $n = 1, \ldots, N$, based on the information from the previously received echo signals of the vehicle. In this paper, we assume that the RSU has established a communication link with the vehicle in time slot 0 [6]–[10]. In the following, we investigate the ISAC-enabled predictive beamforming design stage using an end-to-end deep learning approach.

A. Sensing Model

Let $s_n(t) \in \mathbb{C}$ denote the ISAC downlink signal for the vehicle at time instant t within time slot n. Without loss of generality, we assume $\mathbb{E}\{|s_n(t)|^2\} = 1$. Let $\mathbf{w}_n \in \mathbb{C}^{N_{\mathrm{t}}}$

[1]Without loss of generality, we consider a single vehicle in this work. Our proposed E2E-PB approach can easily be extended to a multi-vehicle scenario. In MIMO mmWave systems, the steering vectors with different AoAs are asymptotically orthogonal. The RSU can distinguish the reflected echo signals from different vehicles with different AoAs and extract the echo signal of each vehicle [6]. Therefore, the beamformers for multiple vehicles can be obtained directly from the signals reflected by the vehicles.

denote the beamforming vector at the RSU in time slot n. The transmitted signal from the RSU can be expressed as

$$\tilde{\mathbf{s}}_n(t) = \mathbf{w}_n s_n(t) \in \mathbb{C}^{N_\mathrm{t}}, \quad 0 \le t \le \Delta T. \tag{3}$$

The reflected echo signals received at the RSU at time instant t within time slot n, $\mathbf{r}_n(t) = [r_{1,n}(t) \ \cdots \ r_{N_\mathrm{r},n}(t)]^\mathrm{T} \in \mathbb{C}^{N_\mathrm{r}}$, are given by

$$\mathbf{r}_n(t) = G\beta_n e^{j2\pi\mu_n t}\mathbf{b}(\theta_n)\mathbf{a}^\mathrm{H}(\theta_n)\tilde{\mathbf{s}}_n(t-\nu_n) + \mathbf{z}_n(t), \tag{4}$$

where $G = \sqrt{N_\mathrm{t}N_\mathrm{r}}$ is the total antenna array gain. ν_n and μ_n are the time delay and Doppler frequency in time slot n, respectively. $\beta_n = \frac{\varrho}{2d_n}$ is the reflection coefficient, where ϱ is the fading coefficient based on the radar cross-section and d_n is the distance between the vehicle and RSU in time slot n. $\mathbf{z}_n(t) \in \mathbb{C}^{N_\mathrm{r}} \sim \mathcal{CN}(\mathbf{0}, \sigma^2\mathbf{I}_{N_\mathrm{r}})$ is the complex Gaussian distributed noise with zero mean and covariance of $\sigma^2\mathbf{I}_{N_\mathrm{r}}$.

B. Observation Model

Given the reflected echo signals $\mathbf{r}_n(t)$ in time slot n, the time delay ν_n and the Doppler frequency μ_n can be estimated by the matched-filtering method [6]:

$$\{\hat{\nu}_n, \hat{\mu}_n\} = \arg\max_{\nu,\ \mu} \left\| \int_0^{\Delta T} \mathbf{r}_n(t) s_n^*(t-\nu) e^{-j2\pi\mu t} dt \right\|^2, \tag{5}$$

where $\hat{\nu}_n$ and $\hat{\mu}_n$ are the estimated values. We can obtain the reflected signal samples[2] $\bar{\mathbf{r}}_n$ from the echo signals as follows:

$$\begin{aligned}
\bar{\mathbf{r}}_n &\triangleq \int_0^{\Delta T} \mathbf{r}_n(t) s_n^*(t-\hat{\nu}_n) e^{-j2\pi\hat{\mu}_n t} dt \\
&= G\beta_n \mathbf{b}(\theta_n)\mathbf{a}^\mathrm{H}(\theta_n)\mathbf{w}_n \\
&\quad \times \int_0^{\Delta T} s_n(t-\nu_n) s_n^*(t-\hat{\nu}_n) e^{-j2\pi(\hat{\mu}_n-\mu_n)t} dt \\
&\quad + \int_0^{\Delta T} \mathbf{z}_n(t) s_n^*(t-\hat{\nu}_n) e^{-j2\pi\hat{\mu}_n t} dt \\
&= G\beta_n \sqrt{\xi}\mathbf{b}(\theta_n)\mathbf{a}^\mathrm{H}(\theta_n)\mathbf{w}_n + \bar{\mathbf{z}}_n,
\end{aligned} \tag{6}$$

where ξ is the matched-filtering gain. $\bar{\mathbf{z}}_n$ is the measured noise in time slot n with zero mean and covariance of $\sigma_\mathrm{r}^2\mathbf{I}_{N_\mathrm{r}}$.

C. Communication Model

From the communication aspect, at time instant $t \in [0, \Delta T]$ in time slot n, the vehicle receives downlink signal from the RSU. The received signal can be expressed as

$$y_n(t) = \tilde{G}\sqrt{\alpha_n} e^{j2\pi\mu_n t}\mathbf{a}^\mathrm{H}(\theta_n)\mathbf{w}_n s_n(t) + \eta_n(t), \tag{7}$$

where $\tilde{G} = \sqrt{N_\mathrm{t}}$ is the antenna gain, $\alpha_n = \alpha_0(d_n/d_0)^{-\zeta}$ is the path loss coefficient, α_0 is the path loss at the reference distance d_0. ζ is the path loss exponent. $\eta_n(t) \sim \mathcal{CN}(0, \sigma_\mathrm{c}^2)$ denotes the complex Gaussian distributed noise at the vehicle with zero mean and variance σ_c^2. The received signal-to-noise ratio (SNR) at the vehicle in time slot n can be expressed as

$$\gamma_n = \frac{|\mathbf{h}_n^\mathrm{H}\mathbf{w}_n|^2}{\sigma_\mathrm{c}^2}, \tag{8}$$

where $\mathbf{h}_n = \tilde{G}\sqrt{\alpha_n}\mathbf{a}(\theta_n)$ is the channel vector between the RSU and the vehicle in time slot n. The achievable rate of the vehicle in time slot n is given by

$$R_n = \log_2(1+\gamma_n) = \log_2\left(1 + \frac{|\mathbf{h}_n^\mathrm{H}\mathbf{w}_n|^2}{\sigma_\mathrm{c}^2}\right). \tag{9}$$

It can be observed from (9) that the achievable rate depends on the transmit beamformer $\mathbf{w}_n$. When the beamformer is perfectly aligned with the channel in the direction of θ_n, the achievable rate is maximized.

D. Problem Formulation

In this paper, we aim to maximize the achievable rate of the vehicle for V2I downlink transmission. The problem of predictive beamforming design in time slot n can be formulated as follows:

$$\underset{\mathbf{w}_n}{\text{maximize}} \ R_n = \log_2\left(1 + \frac{|\mathbf{h}_n^\mathrm{H}\mathbf{w}_n|^2}{\sigma_\mathrm{c}^2}\right) \tag{10a}$$

$$\text{subject to} \ \ \|\mathbf{w}_n\|^2 \le P, \tag{10b}$$

where P denotes the maximum transmit power at the RSU. To solve problem (10), it requires accurate estimation of θ_n or $\mathbf{h}_n$. Some of the related works estimate these two parameters based on mathematical models (e.g., extended Kalman filter [6]) or neural networks (e.g., [9]). Given the estimated parameters, the beamforming vector is determined to maximize the downlink transmission rate. However, the parameters estimation step may introduce errors and the subsequent beamforming design stage does not take the effect of estimation errors into consideration. The achievable rate may be degraded due to error propagation. Motivated by this fact, we propose an end-to-end design to bypass the estimation of state parameters (e.g., θ_n, $\mathbf{h}_n$) and directly target the final goal, i.e., maximizing the achievable rate. Benefiting from the universal approximation capability of neural networks, we propose an E2E-PB approach to learn a mapping between the beamformer and the received signal samples in the previous τ time slots through neural networks.

III. Proposed E2E-PB Approach for V2I Networks

In this section, we present the E2E-PB approach for predictive beamforming design in V2I networks. First, we reformulate problem (10) from an end-to-end learning perspective. Then, we develop an attention-based LSTM network to solve the predictive beamforming problem.

The predictive beamforming problem can be considered as finding a mapping function $\mathcal{F}(\cdot)$, which models the input-output relationship between the reflected signal samples and the beamforming vector under the transmit power constraint. Let matrix $\mathbf{\Gamma}_{n-\tau:n-1} = [\bar{\mathbf{r}}_{n-\tau} \ \cdots \ \bar{\mathbf{r}}_{n-1}]^\mathrm{T} \in \mathbb{C}^{\tau\times N_\mathrm{r}}$ denote the reflected signal samples in the previous τ time slots.

[2]We note that the delay and Doppler frequency compensations are important and common signal processing procedures for sensing [12]. The estimations of ν_n and μ_n are different from the state parameters (e.g., AoA, CSI) estimations. The state parameters estimation step is not required in our proposed approach. The matched-filtering gain and the noise power level are two factors that may affect the performance of predictive beamforming. We will evaluate the effect of these two factors in Section IV.

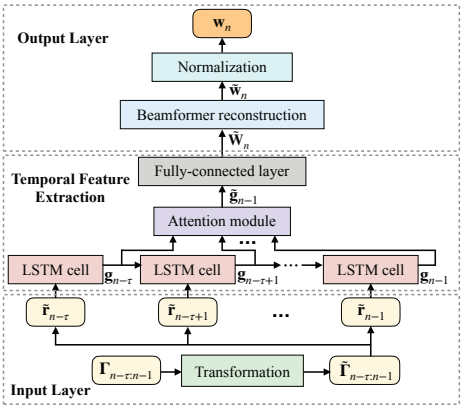

Fig. 3. The proposed attention-based LSTM network.

By characterizing the mapping function with neural networks parameterized by $\mathbf{\Phi}$, i.e., $\mathcal{F}(\cdot\ ;\ \mathbf{\Phi})$, we can reformulate problem (10) as follows:

$$\underset{\mathbf{\Phi}}{\text{maximize}}\ \mathbb{E}_{\mathbf{h}_n}\left\{\log_2\left(1+\frac{|\mathbf{h}_n^{\mathrm{H}}\mathbf{w}_n|^2}{\sigma_{\mathrm{c}}^2}\right)\right\} \tag{11a}$$

$$\text{subject to}\ \ \mathbf{w}_n=\mathcal{F}(\mathbf{\Gamma}_{n-\tau:n-1};\mathbf{\Phi}), \tag{11b}$$

where the expectation $\mathbb{E}\{\cdot\}$ is taken over the channel vector $\mathbf{h}_n$. Since the reflected signal samples are time sequence data, capturing the temporal correlation between the reflected signal samples is important for predictive beamforming design. We develop an attention-based LSTM network to extract the temporal correlation in the reflected signal samples and determine the predictive beamformer, as shown in Fig. 3. The detailed network structure is presented as follows.

1) Input layer: Given the reflected signal samples $\mathbf{\Gamma}_{n-\tau:n-1}$ with dimension $\tau\times N_{\mathrm{r}}$, we can obtain the real and imaginary parts of $\mathbf{\Gamma}_{n-\tau:n-1}$ and concatenate them into a matrix $\tilde{\mathbf{\Gamma}}_{n-\tau:n-1}\in\mathbb{R}^{\tau\times 2N_{\mathrm{r}}}$. The input to the network is given by $\tilde{\mathbf{\Gamma}}_{n-\tau:n-1}$, which is defined as follows:

$$\tilde{\mathbf{\Gamma}}_{n-\tau:n-1}=\left[\mathrm{Re}(\mathbf{\Gamma}_{n-\tau:n-1})\ \mathrm{Im}(\mathbf{\Gamma}_{n-\tau:n-1})\right]. \tag{12}$$

We have $\tilde{\mathbf{\Gamma}}_{n-\tau:n-1}=[\tilde{\mathbf{r}}_{n-\tau}\ \cdots\ \tilde{\mathbf{r}}_{n-1}]^{\mathrm{T}}$, where $\tilde{\mathbf{r}}_l\in\mathbb{R}^{2N_{\mathrm{r}}}$ is the concatenated vector of the real and imaginary parts of $\mathbf{r}_l$, $l=n-\tau,\ldots,n-1$.

2) LSTM cell: The LSTM network can capture both the short-term and long-term temporal dependencies in the input sequences. The LSTM cell takes the concatenated reflected signal samples $\tilde{\mathbf{r}}_l$, $l=n-\tau,\ldots,n-1$, as input, generates the hidden state vector $\mathbf{g}_l$ based on the following operations:

$$\mathbf{f}_l=\sigma\left(\mathbf{W}_f\tilde{\mathbf{r}}_l+\mathbf{U}_f\mathbf{g}_{l-1}+\mathbf{b}_f\right), \tag{13a}$$

$$\mathbf{i}_l=\sigma\left(\mathbf{W}_i\tilde{\mathbf{r}}_l+\mathbf{U}_i\mathbf{g}_{l-1}+\mathbf{b}_i\right), \tag{13b}$$

$$\mathbf{o}_l=\sigma\left(\mathbf{W}_o\tilde{\mathbf{r}}_l+\mathbf{U}_o\mathbf{g}_{l-1}+\mathbf{b}_o\right), \tag{13c}$$

$$\tilde{\mathbf{c}}_l=\tanh\left(\mathbf{W}_c\tilde{\mathbf{r}}_l+\mathbf{U}_c\mathbf{g}_{l-1}+\mathbf{b}_c\right), \tag{13d}$$

$$\mathbf{c}_l=\mathbf{f}_l\odot\mathbf{c}_{l-1}+\mathbf{i}_l\odot\tilde{\mathbf{c}}_l, \tag{13e}$$

$$\mathbf{g}_l=\mathbf{o}_l\odot\tanh\left(\mathbf{c}_l\right), \tag{13f}$$

where $\sigma(\cdot)$ and $\tanh(\cdot)$ denote the sigmoid and hyperbolic tangent activation functions, respectively. $\odot$ represents the Hadamard product. We denote the set $\mathbf{\Phi}_{\mathrm{LSTM}}=\{\mathbf{W}_f,\mathbf{W}_i,\mathbf{W}_o,\mathbf{W}_c,\mathbf{U}_f,\mathbf{U}_i,\mathbf{U}_o,\mathbf{U}_c,\mathbf{b}_f,\mathbf{b}_i,\mathbf{b}_o,\mathbf{b}_c\}$, which includes the weights and biases in the LSTM network. In addition, $\mathbf{f}_l$, $\mathbf{i}_l$, and $\mathbf{o}_l$ are the activation vectors for the forget gate, input gate, and output gate, respectively. $\mathbf{c}_l$ is the cell state vector. The cell state vector and activation vectors are the intermediate vectors generated by the LSTM network, which are used to update the hidden state vector $\mathbf{g}_l$.

3) Attention module: Given an input sequence $\{\tilde{\mathbf{r}}_{n-\tau},\ldots,\tilde{\mathbf{r}}_{n-1}\}$ with length τ, the final hidden state of LSTM $\mathbf{g}_{n-1}$ contains information for the entire input sequence. However, using a single vector $\mathbf{g}_{n-1}$ to represent the information extracted from the sequence $\{\tilde{\mathbf{r}}_{n-\tau},\ldots,\tilde{\mathbf{r}}_{n-1}\}$ may lead to information loss [13]. To tackle this issue, we apply attention mechanism to the hidden states $\{\mathbf{g}_{n-\tau},\ldots,\mathbf{g}_{n-1}\}$, such that the hidden states with more information have larger weights in the output state. The weights are determined by an attention module. In particular, we concatenate the final hidden state $\mathbf{g}_{n-1}$ with $\mathbf{g}_l$, and form the vector $\bar{\mathbf{g}}_{n-1,l}=[\mathbf{g}_{n-1}^{\mathrm{T}}\ \mathbf{g}_l^{\mathrm{T}}]^{\mathrm{T}}$, $l=n-\tau,\ldots,n-1$. We determine the attention weights $a_{n-1,l}$ using the following softmax operation:

$$a_{n-1,l}=\frac{\exp\left\{\mathbf{v}^{\mathrm{T}}\tanh\left(\mathbf{W}_a\bar{\mathbf{g}}_{n-1,l}\right)\right\}}{\sum_{k=n-\tau}^{n-1}\exp\left\{\mathbf{v}^{\mathrm{T}}\tanh\left(\mathbf{W}_a\bar{\mathbf{g}}_{n-1,k}\right)\right\}},\quad l=n-\tau,\ldots,n-1, \tag{14}$$

where $\mathbf{W}_a$ and $\mathbf{v}$ are the parameters of the attention module. We denote the set of parameters in the attention module as $\mathbf{\Phi}_{\mathrm{ATT}}=\{\mathbf{W}_a,\mathbf{v}\}$. Then, the output of the attention module is given by the weighted hidden state vector $\tilde{\mathbf{g}}_{n-1}$:

$$\tilde{\mathbf{g}}_{n-1}=\sum_{l=n-\tau}^{n-1}a_{n-1,l}\mathbf{g}_l. \tag{15}$$

4) Fully-connected layer: We use a fully-connected layer to process the temporal features captured by the previous LSTM layer and the attention module. The sigmoid function is used as the activation function. Let $\mathbf{\Phi}_{\mathrm{FC}}$ denote the parameters of the fully-connected network.

5) Output layer: The output of the fully-connected layer is given by $\tilde{\mathbf{W}}_n\in\mathbb{R}^{N_{\mathrm{t}}\times 2}$, which includes the real and imaginary parts of the obtained beamformer. The beamforming vector $\tilde{\mathbf{w}}_n$ can be determined as follows:

$$\tilde{\mathbf{w}}_n=\tilde{\mathbf{W}}_n[1,:]+j\tilde{\mathbf{W}}_n[2,:], \tag{16}$$

where the first and second terms on the right-hand side are the first and second columns of matrix $\tilde{\mathbf{W}}_n$, respectively. Then, the beamformer is normalized to satisfy the maximum transmit power constraint at the RSU, i.e., $\mathbf{w}_n=\sqrt{P}\tilde{\mathbf{w}}_n/\|\tilde{\mathbf{w}}_n\|$.

We stack the LSTM layer, attention layer, and fully-connected layer together. The set of network parameters is represented as $\mathbf{\Phi}=\{\mathbf{\Phi}_{\mathrm{LSTM}},\mathbf{\Phi}_{\mathrm{ATT}},\mathbf{\Phi}_{\mathrm{FC}}\}$. The loss function is given by

$$\mathcal{L}(\mathbf{w}_n;\mathbf{\Phi})=-\log_2\left(1+\frac{|\mathbf{h}_n^{\mathrm{H}}\mathbf{w}_n|^2}{\sigma_{\mathrm{c}}^2}\right). \tag{17}$$

Algorithm 1 Proposed E2E-PB Approach

Unsupervised Training:

Input: Training dataset $\mathcal{T}_{\text{tr}}$, initialized network parameters $\mathbf{\Phi}^{\text{init}}$, learning rate of the Adam optimizer [14], total number of iterations $N_{\max}$. $N_{\text{iter}} := 0$.

while $N_{\text{iter}} < N_{\max}$ **do**

Sample a batch of data samples from training dataset $\mathcal{T}_{\text{tr}}$.

Update $\mathbf{\Phi}$ to minimize the loss function (17) based on Adam optimizer.

$N_{\text{iter}} := N_{\text{iter}} + 1$.

end while

Output: Trained network parameters $\mathbf{\Phi}^{\star}$.

Online Predictive Beamforming:

Input: Trained network $\mathcal{F}(\cdot\ ;\ \mathbf{\Phi}^{\star})$, test input $\mathbf{\Gamma}^{(\text{ts})}_{n-\tau:n-1}$.

Predictive beamforming based on the trained network $\mathbf{w}_n^{(\text{ts})} = \mathcal{F}(\mathbf{\Gamma}^{(\text{ts})}_{n-\tau:n-1}; \mathbf{\Phi}^{\star})$.

Output: Predicted beamformer $\mathbf{w}_n^{(\text{ts})}$.

We train the proposed network in an unsupervised manner to minimize the loss function (17) using Adam optimizer [14]. We construct a training dataset $\mathcal{T}_{\text{tr}}$ for training. The training dataset contains N_{tr} data pairs of different channel realizations, i.e., $\mathcal{T}_{\text{tr}} = \{(\mathbf{\Gamma}^{(1)}_{n-\tau:n-1}, \mathbf{h}_n^{(1)}), \ldots, (\mathbf{\Gamma}^{(N_{\text{tr}})}_{n-\tau:n-1}, \mathbf{h}_n^{(N_{\text{tr}})})\}$. After training, we can obtain the trained network with parameters $\mathbf{\Phi}^{\star}$ and perform online predictive beamforming. Given the testing data, i.e., the reflected signal samples $\mathbf{\Gamma}^{(\text{ts})}_{n-\tau:n-1}$ as input, we can obtain the predictive beamformer $\mathbf{w}_n^{(\text{ts})}$ from the trained network without estimating the channel vector. The proposed E2E-PB approach is summarized in Algorithm 1.

The computational complexity of the proposed E2E-PB approach is as follows. For the τ-step LSTM module, the computational complexity is $\mathcal{O}(\tau(4D_{\text{i}}D_{\text{o}} + 4D_{\text{o}}^2 + 4D_{\text{o}}))$, where D_{i} and D_{o} are the input and output dimensions of the LSTM cell, respectively. The computational complexity of the attention module is $\mathcal{O}(\tau D_{\text{o}}^2)$. The computational complexity for online beamforming is $\mathcal{O}(\tau(D_{\text{i}}D_{\text{o}} + D_{\text{o}}^2))$. The computational complexity for offline unsupervised training is $\mathcal{O}(S\tau(D_{\text{i}}D_{\text{o}} + D_{\text{o}}^2))$, where S is the number of data samples used for training.

IV. Performance Evaluation

In this section, we evaluate the performance of the proposed E2E-PB approach. Unless stated otherwise, the RSU has $N_{\text{t}} = 32$ transmit antennas and $N_{\text{r}} = 32$ receive antennas. The system is operated at a carrier frequency of 30 GHz. The path loss exponent ζ is set to 3. The fading coefficient ϱ is set to $10 + 10j$. We set σ_{c}^2 to be -100 dBm. The reference distance $d_0 = 1$ m and the path loss at the reference distance is given by $\alpha_0 = -60$ dB [7]. We set $\sigma_{\text{r}}^2 = -60$ dBm and $\xi = 10$ for the observed reflected signal samples. Without loss of generality, the RSU is located at coordinate $[0, 0]$. The distance between the RSU and the road is 10 m. The initial position of the vehicle is randomly located on the road within a range of $[-30, 0]$ on the x-axis. The initial speed of the vehicle is randomly generated from a uniform distribution between $[8, 12]$ m/s. The duration of each time slot ΔT is set to 0.02 s. We set τ to be equal to 6. Based on this system setting, we generated $10,000$ samples, where $8,000$ of them are used for training and the remaining $2,000$ samples are used for testing. The following results are obtained by averaging $2,000$ Monte Carlo realizations in the testing set. For the proposed attention-based LSTM network, the size of the hidden states in LSTM cell, the size of the attention network parameters, and the number of neurons in the fully-connected layer are set to 256. The Adam optimizer is used for training the network with a learning rate of 10^{-4}.

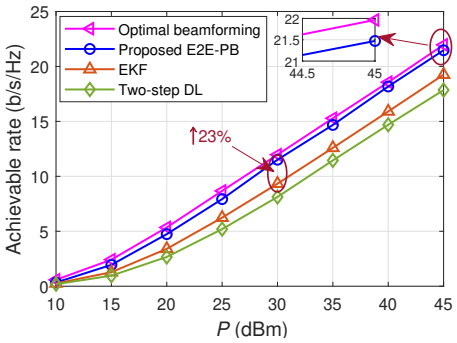

Fig. 4. The achievable rate of the vehicle versus the maximum transmit power P at the RSU ($N_{\text{t}} = N_{\text{r}} = 32$).

For performance comparison, we include the following three methods as benchmarks:

- Optimal beamforming design with perfect CSI (Optimal beamforming): When CSI $\mathbf{h}_n$ is available at the RSU, the optimal beamformer is given by $\mathbf{w}_n^{\star} = \mathbf{h}_n$. In this case, the vehicle can obtain the maximum achievable rate.
- Extended Kalman filter (EKF) [6]: The EKF approach first estimates θ_n based on a mathematical model, which describes the kinematic relationship between θ_n, the speed of the vehicle, as well as the distance between the vehicle and the RSU. The beamformer is then determined based on the estimated θ_n.
- Deep learning based two-step approach (Two-step DL) [9]: This approach first extracts the angular information of the previous time slots from the reflected signal samples using deep learning. The value of θ_n is predicted based on historical angular information. The beamformer is then obtained based on θ_n.

In Fig. 4, we show the achievable rate versus the maximum transmit power P at the RSU. We can observe from Fig. 4 that the proposed E2E-PB approach outperforms the EKF and the two-step DL schemes. In particular, when P is equal to 30 dBm, the proposed approach can improve the achievable rate up to 23% when compared with the EKF approach. The results show the advantages of the proposed end-to-end learning approach, which bypasses the state parameters estimation step. Moreover, when P is equal to 45 dBm, the proposed E2E-PB approach can achieve over 97% of the achievable rate of the optimal beamforming design with perfect CSI. This indicates the effectiveness of the proposed attention-based LSTM network, which can capture the most important temporal features from the reflected signal samples.

In Fig. 5, we show the achievable rate versus the number of

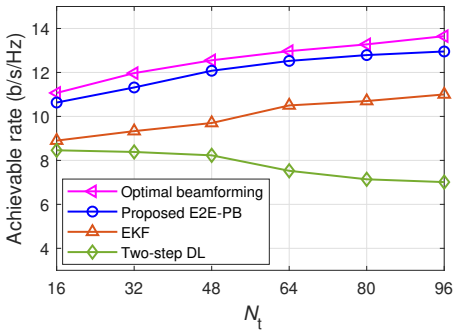

Fig. 5. The achievable rate of the vehicle versus the number of transmit antennas N_t at the RSU ($P = 30$ dBm, $N_r = N_t$).

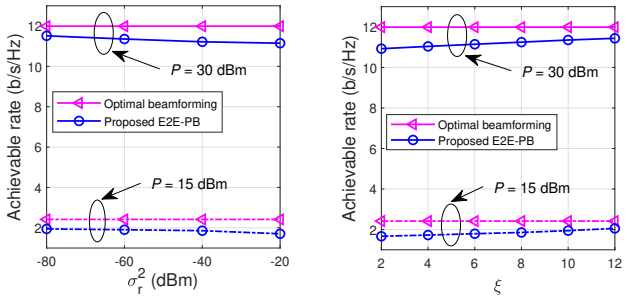

Fig. 6. Effect of (a) the noise level σ_r^2 and (b) the matched-filtering gain ξ in the received signal samples on the achievable rate ($N_t = N_r = 32$).

transmit antennas N_t, where the number of receive antennas N_r is equal to N_t. Results show that the proposed E2E-PB approach leads to a steady increase in the achievable rate when the number of antennas increases. It obtains over 96% of the achievable rate of the optimal beamformer with perfect CSI. On the other hand, the two-step DL approach suffers performance degradation with an increasing number of antennas. This is due to the fact that the two-step DL approach aims at minimizing the estimation error of the historical spatial angles in the first step. The impact of the estimation error is not taken into account when designing the predictive beamformer. In this case, the obtained beamformer may deviate from the true angular direction. As the number of antennas increases, the formed beam becomes narrow, such that the angular deviation may lead to more significant performance degradation.

In Fig. 6, we evaluate the effect of σ_r^2 and ξ in (6) on the achievable rate of the proposed E2E-PB approach. It can be observed that different values of σ_r^2 and ξ have a slight impact on the performance of the proposed E2E-PB approach. This demonstrates the robustness of the proposed approach against the noise power and matched-filtering gain. This is because the proposed attention-based LSTM network has the capability to tackle the uncertainty caused by the noise in the signals.

V. Conclusion

In this paper, we investigated the ISAC-enabled predictive beamforming design for V2I networks. Different from existing works which exploit two-step approaches to design the beamformer, we proposed an end-to-end approach that bypasses the intermediate state parameters estimation step. The proposed E2E-PB approach can directly obtain the predictive beamformer from the reflected signal samples. An attention-based LSTM network was developed to extract the temporal correlation from the reflected signal samples and determine the beamforming vector. The network is trained in an unsupervised manner which aims to maximize the achievable rate. Simulation results showed that the proposed E2E-PB approach outperforms two baseline schemes, namely, EKF [6] and the two-step DL [9]. Results also showed that the proposed approach achieves close-to-optimal performance when compared with the optimal beamforming design with perfect CSI. For future work, we will provide a generalized framework of end-to-end beamforming design for joint localization, communication, and tracking with the aid of ISAC.

References

[1] Z. Zhang, Y. Xiao, Z. Ma, M. Xiao, Z. Ding, X. Lei, G. K. Karagiannidis, and P. Fan, "6G wireless networks: Vision, requirements, architecture, and key technologies," *IEEE Veh. Tech. Mag.*, vol. 14, no. 3, pp. 28–41, Sept. 2019.

[2] H. Tataria, M. Shafi, A. F. Molisch, M. Dohler, H. Sjöland, and F. Tufvesson, "6G wireless systems: Vision, requirements, challenges, insights, and opportunities," *Proc. of the IEEE*, vol. 109, no. 7, pp. 1166–1199, Jul. 2021.

[3] K. B. Letaief, W. Chen, Y. Shi, J. Zhang, and Y.-J. A. Zhang, "The roadmap to 6G: AI empowered wireless networks," *IEEE Commun. Mag.*, vol. 57, no. 8, pp. 84–90, Aug. 2019.

[4] F. Liu, Y. Cui, C. Masouros, J. Xu, T. X. Han, Y. C. Eldar, and S. Buzzi, "Integrated sensing and communications: Toward dual-functional wireless networks for 6G and beyond," *IEEE J. Sel. Areas in Commun.*, vol. 40, no. 6, pp. 1728–1767, Jun. 2022.

[5] A. Liu, Z. Huang, M. Li, Y. Wan, W. Li, T. X. Han, C. Liu, R. Du, D. K. P. Tan, J. Lu, Y. Shen, F. Colone, and K. Chetty, "A survey on fundamental limits of integrated sensing and communication," *IEEE Commun. Surveys & Tuts.*, vol. 24, no. 2, pp. 994–1034, 2nd Quat. 2022.

[6] F. Liu, W. Yuan, C. Masouros, and J. Yuan, "Radar-assisted predictive beamforming for vehicular links: Communication served by sensing," *IEEE Trans. on Wireless Commun.*, vol. 19, no. 11, pp. 7704–7719, Nov. 2020.

[7] W. Yuan, F. Liu, C. Masouros, J. Yuan, D. W. K. Ng, and N. González-Prelcic, "Bayesian predictive beamforming for vehicular networks: A low-overhead joint radar-communication approach," *IEEE Trans. on Wireless Commun.*, vol. 20, no. 3, pp. 1442–1456, Mar. 2021.

[8] F. Liu and C. Masouros, "A tutorial on joint radar and communication transmission for vehicular networks – Part III: Predictive beamforming without state models," *IEEE Commun. Lett.*, vol. 25, no. 2, pp. 332–336, Feb. 2021.

[9] J. Mu, Y. Gong, F. Zhang, Y. Cui, F. Zheng, and X. Jing, "Integrated sensing and communication-enabled predictive beamforming with deep learning in vehicular networks," *IEEE Commun. Lett.*, vol. 25, no. 10, pp. 3301–3304, Oct. 2021.

[10] C. Liu, W. Yuan, S. Li, X. Liu, H. Li, D. W. K. Ng, and Y. Li, "Learning-based predictive beamforming for integrated sensing and communication in vehicular networks," *IEEE J. Sel. Areas in Commun.*, vol. 40, no. 8, pp. 2317–2334, Aug. 2022.

[11] C. B. Barneto, S. D. Liyanaarachchi, M. Henino, T. Riihonen, and M. Valkama, "Full duplex radio/radar technology: The enabler for advanced joint communication and sensing," *IEEE Wireless Commun.*, vol. 28, no. 1, pp. 82–88, Feb. 2021.

[12] G. Hakobyan and B. Yang, "High-performance automotive radar: A review of signal processing algorithms and modulation schemes," *IEEE Signal Process. Mag.*, vol. 36, no. 5, pp. 32–44, Sept. 2019.

[13] D. Bahdanau, K. Cho, and Y. Bengio, "Neural machine translation by jointly learning to align and translate," in *Proc. Int. Conf. Learn. Representations (ICLR)*, San Diego, CA, May 2015.

[14] D. P. Kingma and J. L. Ba, "Adam: A method for stochastic optimization," in *Proc. Int. Conf. Learn. Representations (ICLR)*, San Diego, CA, May 2015.